

Non-Doppler shift related experimental shock wave measurements using velocity interferometer systems for any reflector

A. C. Forsman and G. A. Kyrala

Los Alamos National Laboratory, Los Alamos, New Mexico 87545

(Received 3 October 2000; published 17 April 2001)

Velocity interferometer system for any reflectors (VISARs), are becoming increasingly popular in the measurement of shock waves in solids and liquids. VISAR techniques are used in measurements of transit time, speed of shock waves in flight in transparent media [L. C. Chhabildas and J. L. Wise, in *Proceedings of the 4th APS Topical Conference on Shock Waves in Condensed Matter, Spokane, Washington, 1985*, edited by Y. M. Gupta (Plenum, New York, 1986); P. M. Celliers *et al.*, *Appl. Phys. Lett.* **73**, 1320 (1998)], and in measurements of particle velocity. However, in cases where shock compression or release may change the index of refraction $n + ik$ of the material being studied, the VISAR technique must be applied with care. Changes in n and k introduce phase shifts into the VISAR results that are not associated with changes in velocity. This paper presents a derivation of the theoretical output of a line VISAR that includes the effects of changing n and k and an experimental observation of a non-Doppler shift related effect.

DOI: 10.1103/PhysRevE.63.056402

PACS number(s): 52.35.Tc, 62.50.+p

Velocity interferometer system for any reflector (VISAR) measurements are typically designed to be sensitive to the changes in the velocity of a reflecting surface on a moving target. In the vast majority of the existing body of work the material state of the reflecting surface itself undergoes little, if any, change [1–5]. However, recent advances in equation-of-state studies involve the use of VISARs to measure the velocities of shocked surfaces at multimegabar pressures and in nonmetallic media [2]. These are both significant departures from many of the traditional experimental conditions diagnosed by VISARs and as such a close examination of the effects of changing reflective properties is warranted. This paper addresses the relation of nonvelocity related changes in targets to the apparent velocities of those targets as measured using streaked optical imaging VISARs. The type of VISAR considered is shown in Fig. 1, where the light reflected from the target enters the VISAR and is directed along two paths having different optical path lengths. The light is then recombined at the output beam splitter, which is also where an image of the target is formed. This image is then relayed onto the slits of optical streak cameras to record the measurement. The optical path length difference is customarily expressed as a delay time, and for this reason the path length difference will be referred to as $c\tau$, where c is the speed of light and τ is the delay time.

In order to facilitate interpretation, the user frequently imposes fringes on the output beam splitter by giving the output beam splitter a slight tilt. In the treatment in this paper, tilt is included through the parameters Ω and y , where

$$\Omega = \frac{2\pi \sin \theta}{\lambda}. \quad (1)$$

The probe-laser wavelength is λ , θ is the angular excursion from the position of the output beam splitter that would yield the perfect “bull’s-eye” in the interference pattern, and y is the distance across the surface of the beam splitter.

The interference pattern formed at the output beam splitter can be expressed as

$$I = E^* E, \quad (2)$$

where

$$E = E_L e^{-i(\Omega y + \phi_L)} + E_S e^{-i(-\Omega y + \phi_S)}. \quad (3)$$

E is electric field and the subscripts L and S refer to the light arriving at the output beam splitter from the long and short paths, respectively. An approximation involved here is that the imposed fringe term constant Ω will not change significantly for Doppler-shifted light. This is a good approximation since the total path length change $y \sin \theta$ is several wavelengths, much smaller than the several millimeter to several centimeter lengths typical of $c\tau$.

ϕ_L and ϕ_S bear close examination. They represent the remaining contributions to the phase of the light at the output beam splitter. Owing to the presence of the optical delay element, the light coming through the long arm is delayed by the time τ . Thus,

$$\begin{aligned} \phi_L(t) &= \int_0^t \frac{d\phi}{dt'} \Big|_{t'-\tau} dt', \\ \phi_S(t) &= \int_0^t \frac{d\phi}{dt'} \Big|_{t'} dt', \end{aligned} \quad (4)$$

$$\Delta\phi(t) = \phi_S(t) - \phi_L(t).$$

The initial time $t=0$ is arbitrary. It simply refers to a time before anything has happened to the target. If we use these expressions for the phases in Eqs. (2) and (3) to calculate the intensity distribution we get

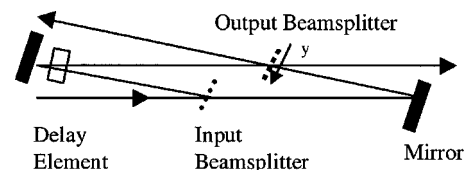


FIG. 1. Schematic drawing of the VISAR used in the present work.

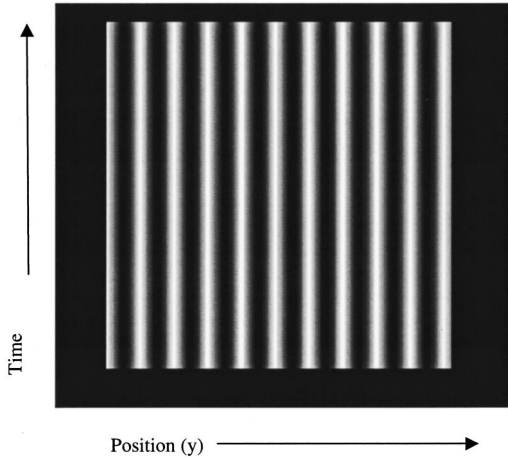


FIG. 2. Simulation of streak camera record of VISAR output produced by a steady-state target.

$$I(t, y) = E_0^2 \{2 + 2 \cos[2\Omega y + \Delta\phi(t)]\}. \quad (5)$$

This expression assumes that the effects of the beam splitters are equal. In order to illustrate the way that velocity and material property changes of the reflecting surface affect the interpretation of VISAR results, we perform three case studies of the temporal behavior of the VISAR output.

First, there is the steady-state condition. By steady state, we refer to a target at constant velocity and unchanging surface condition. Therefore,

$$\frac{d\phi}{dt'} = \frac{2\pi c}{\lambda}.$$

Since the target is in a steady state, time dependence vanishes and the expression for intensity, Eq. (5), is thus

$$I(t, y) = I(y) = E_0^2 [2 + 2 \cos(2\Omega y)]. \quad (6)$$

This is the pattern we record when this VISAR is being aligned and is plotted in Fig. 2.

The second case is that of simple acceleration [5]. By simple acceleration, we refer to a target that changes instantaneously to a different velocity v but undergoes no other changes. Let us, for convenience, define a as the time when the Doppler-shifted light arrives at the output beam splitter of the VISAR through the short arm of the interferometer. Then Eq. (5) is

$$\Delta\phi_D(t) = 2\pi c \int_0^t \left[\frac{1}{\lambda_{t'-\tau}} - \frac{1}{\lambda_{t'}} \right] dt', \quad (7)$$

$$I(t, y) = E_0^2 \{2 + 2 \cos[2\Omega y + \Delta\phi_D(t)]\}.$$

The subscript D has been added to the time-dependent term since in this case the phase shifts arise from a Doppler shift in the light reflected from the target. The contribution $\Delta\phi_D$ develops between the time a and $a + \tau$. Thus,

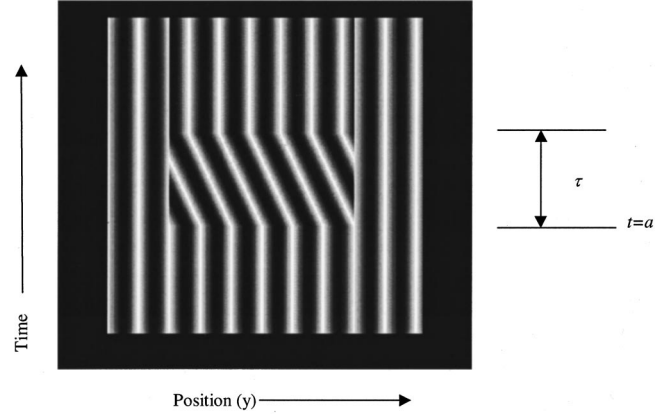


FIG. 3. Simulated streak camera record of VISAR output corresponding to simple acceleration. Only the central portion of the target is being accelerated. The total sideways fringe shift is $\Delta\phi_D$.

$$\Delta\phi_D(t) = 0, \quad t < a,$$

$$\Delta\phi_D(t) = 2\pi c \int_a^{a+t} \left[\frac{1}{\lambda_{t'-\tau}} - \frac{1}{\lambda_{t'}} \right] dt', \quad a < t < a + \tau, \quad (8)$$

$$\Delta\phi_D(t) = 2\pi c \left(\frac{1}{\lambda} - \frac{1}{\lambda'} \right) \tau, \quad t > a + \tau,$$

where λ' is the wavelength of the Doppler-shifted light.

This expression is plotted in Fig. 3 and shows that as time proceeds from the beginning of the experiment to the time at which the Doppler-shifted light arrives at the output beam splitter, no fringe shifts will be observed. Then, as the Doppler-shifted light arrives at the beam splitter from the short arm but not from the long arm, a linearly increasing fringe shift will be observed. A simple method of visualizing this process is to consider two hypothetical phase meters at the output beam splitter, one registering ϕ_L and the other registering ϕ_S . When both meters are seeing light of equal wavelength arriving at the beam splitter, both meters advance at the same rate. However, since the Doppler-shifted light arrives first through the short arm, then for a time τ , ϕ_S advances at a faster rate, and the resulting phase difference appears in the VISAR output as a fringe shift. After the time interval τ the Doppler-shifted light propagates through the long arm as well and then the two phase meters once again advance at a common rate, so no further fringe shifting is observed.

The third case is a change of material properties. For the sake of discussion, the target instantaneously undergoes changes in velocity and in n and k and the time $t = a$. Then, there are two time dependent terms in the VISAR output equation, $\Delta\phi_D$ and $\Delta\phi_R$, where ϕ_R is the change of phase upon reflection.

$$\Delta\phi_R(t) = [\phi_R|_{t>a} - \phi_R|_{t<a}] \times \int_0^t [\delta(t' - \tau - a) - \delta(t' - a)] dt', \quad (9)$$

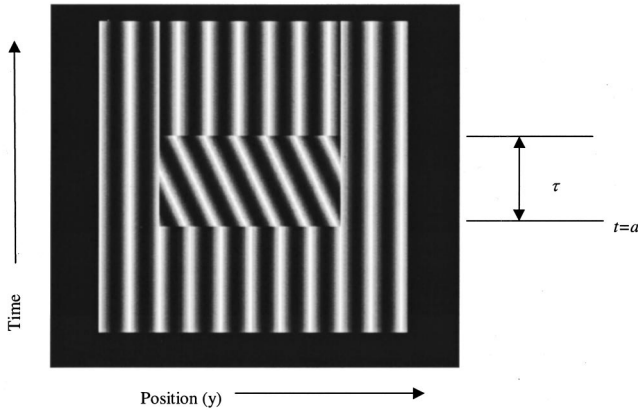


FIG. 4. Simulated streak camera record of VISAR output corresponding to a target that is simultaneously accelerated and subject to changes in material properties. The sideways discontinuity is $\Delta\phi_R$.

where ϕ_R changes at time $t=a$ since that is when the material properties of the target change. Thus Eq. (5) becomes

$$I(t, y) = E_0^2 \{2 + 2 \cos[2\Omega y + \Delta\phi_D(t) + \Delta\phi_R(t)]\}. \quad (10)$$

This obviously gives rise to a transient effect whose duration is equal to τ and whose magnitude is equal to the change in the change of phase upon reflection of light from the target. This is plotted in Fig. 4. This easily fits into the phase meter argument since the sudden change in phase of reflection arising from the change in material properties may be viewed as putting a discontinuity in the wave train reflected from the target. Therefore, when this discontinuity reaches the output beam splitter via the short arm, that phase meter moves ahead a discrete amount and the transient feature appears. When the discontinuity reaches the output beam splitter via the long arm, that phase meter moves ahead the same discrete amount, causing the transient feature to disappear.

In the foregoing illustration, changes in the phase of the reflected light were treated as step functions. In actual practice changes occur over some time. Figure 5 shows the VISAR record from $a \cong 140$ kbar shock emerging from a silicon wafer. The shock is driven through the 20- μm -thick wafer by a 1.8-ns laser pulse. One-half of the silicon wafer is coated with 1000 \AA of aluminum. There are two salient features to this figure. The time scale of the VISAR response is 70 ps, slightly longer than the streak camera response time.

At time $t=0$ the fringes start moving to the right. On the aluminized side, they move and reach a new, final, position. On the bare silicon side they move right, and then back part-way to the left at $t=150$ ps.

The differences between the two sets of fringes can be qualitatively understood by considering the pressure induced band gap closure in silicon at 140 kbar and the process of shock wave arrival at and rarefaction wave propagation into the surface of the silicon wafer. Following band-gap closure [6], the shocked silicon may be considered to be in a metallic state. Upon arrival at the surface of the wafer, an optical probe will be reflecting from a metallic state instead of a semiconducting state. This means that the phase change upon

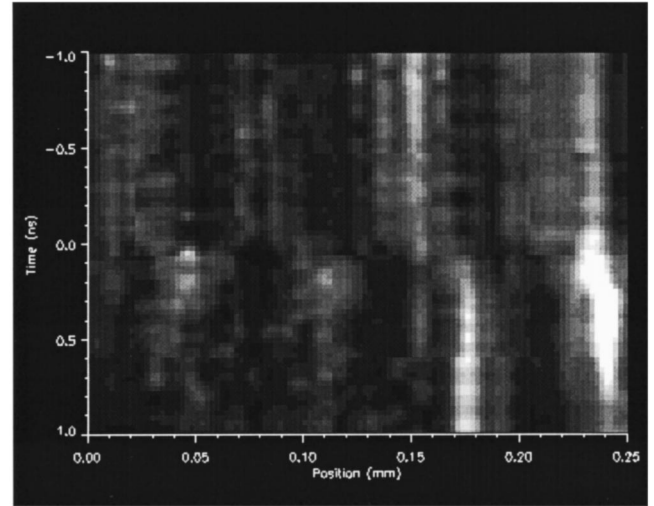


FIG. 5. Streak camera record of shock wave breakout from silicon. Left half, bare silicon. Right half, aluminized silicon. Shock breakout is at zero time. These images have been subject to slight image processing [9] to reduce the noise arising from pixelation. The sensitivity is 4.9 km/s fringe.

reflection from the silicon wafer is going to undergo a different change from the phase change upon reflection from the preshocked state of the wafer. To establish an order-of-magnitude estimate of the change in phase due only to the change in state of the silicon, we employ Fresnel's equation

$$R = \left(\frac{1 - (n + ik)}{1 + (n + ik)} \right), \quad (11)$$

where R will be a complex quantity containing phase and magnitude information. For red (660 nm) light the index of refraction for normal, unshocked, silicon [7] is $3.8 + i0.016$, and we will use the values of aluminum, $1.5 + i7.8$, for shocked silicon. The usage of aluminum data for metallic silicon is acceptable for estimation since the electron densities, mass densities, ionization states, and electrical conductivities [8] are similar. According to the preceding equation, the change of phase upon reflection for normal silicon is 0.3° and the change of phase upon reflection of the metallic silicon (aluminum, in our estimate) is 194° . In the absence of any other processes such as shock release, this change will manifest itself as a shift of slightly more than one-half of one fringe.

In the case of the present data, how this phase change manifests itself is a function of both the skin depth of the unshocked silicon, approximately 1 μm , and the breakout of the shock wave. Both the phase and the wavelength of the reflected-probe light will change as the shock wave crosses through the skin depth to the free surface. During this transit time, typically <1 ns, the reflected light interacts with the vacuum-silicon interface, the metallic shocked silicon, and the intervening unshocked silicon. Although reflection in this case is a nonlocal phenomenon, the short (<70 ps) rise time of the shock breakout signal suggests that the reflection is dominated by the vacuum-silicon interface rather than by the shocked-unshocked material interface. When the shock wave

arrives at the vacuum silicon interface, the light will be reflecting from a metallic surface. The higher reflectivity of this state is evident in the data as an increase in the reflectivity at the time of the shock breakout, the duration of which is determined by a convolution of the target reflectivity history and instrumental response. Immediately following the arrival of the shock wave at the surface, a rarefaction wave sets in and the silicon relaxes to a lower pressure nonmetallic state and will be moving outward at twice the speed of the shock-compressed material. This quickly obscures the metallic state.

The fringes from the aluminized portion of the target do not show any “slowing down” or changing response rates. This contrast with the bare silicon data show that only by considering the effects of changing material states on the phase of the reflected light, can the features of the data be explained.

Non-Doppler effects in VISAR measurements manifest themselves on time scales less than the delay time inherent in the VISAR and have been observed in silicon shock waves in the present work. It is beyond the scope of the present work to list all possible circumstances in which non-Doppler

effects will appear, but two potential cases are worth mentioning here. First, in applying the VISAR to the study of high pressure free-surface shock wave releases, where the target surface disassembles on time scales that are of the order of or shorter than the VISAR delay element time τ , one would expect a series of overlapping transients. In such a situation, extracting the velocity information is not necessarily straightforward. The importance of these transients to the final fringe shift also depends on the fringe constant of the VISAR. The second case involves the use of transparent windows to prevent a free-surface release of the shock wave. If one chooses a time delay τ longer than the response of the optical recording system but shorter than the time required for the shock to transit the window, then observation of a fringe structure like the one shown in Fig. 4 becomes possible. Hence, a measurement of the changes in the index of refraction and consequently the electronic properties of the shock-compressed materials would be obtained.

This work was performed under the auspices of the U.S. Department of Energy under Contract No. W-7405-ENG-36.

-
- [1] L. C. Chhabildas and J. L. Wise, in *Proceedings of the 4th APS Topical Conference on Shock Waves in Condensed Matter, Spokane, Washington, 1985*, edited by Y. M. Gupta (Plenum, New York 1986).
- [2] P. M. Celliers, G. W. Collins, L. B. Da Silva, D. M. Gold, and R. Cauble, *Appl. Phys. Lett.* **73**, 1320 (1998).
- [3] L. M. Barker and R. E. Hollenbach, *J. Appl. Phys.* **43**, 4669 (1972).
- [4] D. L. Paisley, R. H. Warnes, and R. A. Kopp, in *Shock Compression of Condensed Matter—1991*, edited by S. C. Schmidt *et al.* (Elsevier Science, New York, 1992), pp. 825–828; D. L. Paisley, in *Shock-Wave and High-Strain Rate Phenomena in Materials EXPLOMET*, edited by M. C. Meyers *et al.* (Dekker, New York, 1992).
- [5] W. F. Hemsing, in *Proceedings of SPIE Optical and Optoelectronic Applied Science and Engineering, San Diego, 1990*, edited by L. L. Shaw, P. A. Jaanimagi, and B. T. Meyer (SPIE, Bellingham, WA, 1991).
- [6] N. F. Mott, *Metal-Insulator Transitions* (Barnes & Noble, New York, 1974.)
- [7] J. P. Weaver and H. P. R. Frederikse, *Handbook of Chemistry and Physics, 78th ed.* (Chemical Rubber Company, New York, 1998).
- [8] Y. T. Lee and R. M. More, *Phys. Fluids* **27**, 1273 (1984).
- [9] R. K. Keinigs, J. E. Hammerberg, and G. Kyrala, Report No. LA-UR-98-4080 (unpublished); W. H. Press, B. P. Flannery, S. A. Teukolsky, and W. T. Vetterling, *Numerical Recipes* (Cambridge University Press, Cambridge, 1986).